# The gross theory model for neutrino-nucleus cross-section

New Journal of Physics
The open-access journal for physics

# The gross theory model for neutrino-nucleus cross-section

**A R Samana[1,2], C A Barbero[3,4,8], S B Duarte[2], A J Dimarco[5] and F Krmpotić[3,6,7]**

[1] Department of Physics, Texas A&M University—Commerce, PO Box 3011, Commerce, TX, USA
[2] Centro Brasileiro de Pesquisas Físicas, Rua Dr Xavier Sigaud 150, CEP 22290-180, Rio de Janeiro-RJ, Brazil
[3] Instituto de Física La Plata, CONICET, 1900 La Plata, Argentina
[4] Departamento de Física, Facultad de Ciencias Exactas, Universidad Nacional de La Plata, CC 67, 1900 La Plata, Argentina
[5] Departamento de Ciências Exactas e Tecnológicas, Universidade Estadual de Santa Cruz, CEP 45662-000 Ilheús, Bahia-BA, Brazil
[6] Departamento de Física Matemática, Instituto de Física da Universidade de São Paulo, Caixa Postal 66318, 05315-970 São Paulo-SP, Brazil
[7] Facultad de Ciencias Astronómicas y Geofísicas, Universidad Nacional de La Plata, 1900 La Plata, Argentina
E-mail: arturo@cbpf.br and barbero@fisica.unlp.edu.ar

*New Journal of Physics* **10** (2008) 033007 (17pp)
Received 7 November 2007
Published 6 March 2008
Online at http://www.njp.org/
doi:10.1088/1367-2630/10/3/033007

**Abstract.** The nuclear gross theory, originally formulated by Takahashi and Yamada (1969 *Prog. Theor. Phys.* **41** 1470) for the $\beta$-decay, is applied to the electronic-neutrino nucleus reactions, employing a more realistic description of the energetics of the Gamow–Teller resonances. The model parameters are gauged from the most recent experimental data, both for $\beta^-$-decay and electron capture, separately for even–even, even–odd, odd–odd and odd–even nuclei. The numerical estimates for neutrino-nucleus cross-sections agree fairly well with previous evaluations done within the framework of microscopic models. The formalism presented here can be extended to the heavy nuclei mass region, where weak processes are quite relevant, which is of astrophysical interest because of its applications in supernova explosive nucleosynthesis.

[8] Author to whom any correspondence should be addressed.

## Contents



## 1. Introduction

The nucleosynthesis of heavy elements is only understood if stellar reactions take place in regions of the nuclear chart far away from the $\beta$-stability line, involving a large number of unstable or even exotic nuclear species for which experimental data are very scarce. For instance, the steps of nucleosynthesis in the $r$-process occur outside and just along the neutron drip line, many of the principal nuclear properties of which are still unknown. A great deal of theoretical and experimental efforts have been made in the last few decades in order to describe the nuclear properties of different species along the $\beta$-stability line, as well as those of exotic nuclei involved in explosive nucleosynthesis processes [1]–[3].

The theoretical models can be divided generically into: (i) the macroscopic models which describe the global nuclear properties ([4]–[6]; [7] and references therein [8]–[10]), where special attention is paid to the *gross theory of the $\beta$-decay* (GTBD); and (ii) the microscopic formalisms i.e. the shell model or random phase approximation (RPA) based calculations [10]–[13], where the detailed nuclear structure of each species is considered.

The GTBD was first proposed by Takahashi and Yamada [4] nearly 40 years ago to describe the global properties of allowed $\beta$-decay processes. It is essentially a parametric model, which attempted to combine the single-particle and statistical arguments in a phenomenological way. Later, different versions of the 'gross theory' were developed and have been used for practical applications very frequently [5]–[9]. This is due to: (i) their simplicity when compared with the hard computational work involved in the implementation of the microscopic models and (ii) their capability to reproduce the available experimental data and to be extrapolated later on to unknown nuclei far away from the $\beta$-stability line. In fact, as these theoretical approaches account systematically and fairly well for the properties of stable nuclei, they have been extensively applied to describe: (i) the $\beta$-decay half-lives and other nuclear observables participating in the $r$-process and (ii) the properties of a great number of exotic nuclei that are involved in the nucleosynthesis.

It should also be mentioned that the gross-theory approach has also been used by Itoh *et al* [14] for the calculation of the total capture of a neutrino by $^{37}$Cl, $^{16}$O, $^{20}$Ne and $^{56}$Fe nuclei, which are used in the detection of solar neutrinos.

The aim of the present work is twofold. Firstly, motivated by the simplicity of the original GTBD, we use it to evaluate the half-lives of allowed weak-transitions ($\beta$-decay and electron-capture) in nuclei with $A < 70$, which are of major importance in presupernova collapse processes. We also analyze the consequences of employing a more realistic estimate in this study for the energetics of the Gamow–Teller resonance (GTR) than in the previous works. This will lead us to a new trend for the adjustable parameter related to the energy spread of the GTR caused by the spin-dependent part of the nuclear force. Secondly, we use the same gross-theory approach to describe the nuclear neutrino capture over a large number of nuclei involved in the presupernova structure with the purpose of extending, in the future, the calculation to the $r$-process in a neutrino-rich environment. Since within the stellar conditions no experimental data exist, our results are compared with those achieved in the framework of microscopic approaches.

The paper is organized as follows. In section 2, we briefly sketch the conventional gross theory for nuclear $\beta$-decay and electron-capture rate. In section 3, we introduce the gross theory for the evaluation of the neutrino-nucleus reaction cross-section. The single-particle strength functions are discussed in sections 4 and 5, together with the estimate of the GTR energy and the procedure used to derive the corresponding spread of the transition strength. In section 6, we present and discuss our results. The conclusions drawn and future extensions of the present work are given in section 7.

## 2. The gross theory of nuclear $\beta$-decay (GTBD)

The GTBD permits us to evaluate the half-lives of $\beta^{\pm}$-decay and the rates for electron capture weak processes. As an example, we briefly sketch here the original GTBD [4] for the decay $(Z, A) \rightarrow (Z+1, A) + e^- + \bar{\nu}$. The total rate for allowed transitions is written (in natural units) as

$$\lambda_\beta = \frac{G_F^2}{2\pi^3} \int_{-Q_\beta}^{0} dE \left[ g_V^2 |\mathcal{M}_F(E)|^2 + g_A^2 |\mathcal{M}_{GT}(E)|^2 \right] f(-E), \tag{1}$$

where $G = (3.034545 \pm 0.00006) \times 10^{-12}$ is the Fermi weak coupling constant, $g_V = 1$ and $g_A = -1$ are, respectively, the vector and axial-vector effective coupling constants[9]. The argument of the matrix element $(E)$ is the transition energy measured from the parent ground state. Note that the true $\beta$-decay transition energy is $E_\beta = E_e + E_\nu = -E > 0$. The usual integrated dimensionless Fermi function [15, 16], $f(E)$, is evaluated from the approximated formulae given in [4] that are correct up to ~10% for standard decays. The $Q_\beta$-value is the difference between neutral atomic masses of parent and daughter nuclei:

$$Q_{\beta^-} = M(A, Z) - M(A, Z+1) = B(A, Z+1) - B(A, Z) + m(\mathrm{nH}) \tag{2}$$

with $B(A, Z)$ and $B(A, Z+1)$ being the corresponding nuclear binding energies, and $m(\mathrm{nH}) = m_n - m(^1\mathrm{H}) = m_n - m_p - m_e = 0.782\,\mathrm{MeV}$. The masses were obtained in the same way as in [7]. This means that, when available, they are taken from the Wapstra–Audi–Hoekstra mass table [17] and, otherwise, they are determined from the Tachibana–Uno–Yamada semi–empirical mass formula [18].

[9] Finite nuclear size effects are incorporated via the dipole form factor $g \rightarrow g\left(\frac{\Lambda^2}{\Lambda^2+k^2}\right)$, where $k$ is the momentum transfer and $\Lambda = 850\,\mathrm{MeV}$ the cutoff energy.

The squares of the Fermi (F) and Gamow-Teller (GT) matrix elements are determined as:

$$|\mathcal{M}_X(E)|^2 = \int_{\epsilon_{\min}}^{\epsilon_{\max}} D_X(E,\epsilon) W(E,\epsilon) \frac{\mathrm{d}n_1}{\mathrm{d}\epsilon} \mathrm{d}\epsilon, \qquad \text{for } X = \mathrm{F}, \mathrm{GT}. \tag{3}$$

Here, $\epsilon_{\min}$ is the lowest single-particle energy of the parent nucleus and $\epsilon_{\max}$ is the energy of the highest occupied state. The one-particle-level density (proton or neutron), $\mathrm{d}n_1/\mathrm{d}\epsilon$, is determined by the Fermi gas model for the parent nucleus, and the weight function $W(E,\epsilon)$, constrained by $0 \leqslant W(E,\epsilon) \leqslant 1$, takes into account the Pauli blocking. Finally, $D_X(E,\epsilon)$, normalized as $\int_{-\infty}^{+\infty} D_X(E,\epsilon)\,\mathrm{d}E = 1$, is the probability that a nucleon with single-particle energy $\epsilon$ undergoes a $\beta$-transition. As in [4] we neglect the $\epsilon$-dependence, i.e. it is assumed that all nucleons have the same decay probability, independent of their energies $\epsilon$, $D_X(E,\epsilon) \equiv D_X(E)$. The GTBD characterizes this $D_X(E)$ through their energy weight moments (for example, in [14] these expressions were written explicitly).

The dependence on the odd–even proton and neutron numbers in the daughter nucleus is introduced through the values for the pairing gap $\Delta$ and the single-particle level spacing $d$. In the present work, we adopted those from [5]. More details of the probability function $D_X(E)$ are given in section 4.

The original GTBD [4] has been gradually improved [6, 7], and nowadays we have two new versions: the first is named the 2nd generation gross theory (GT2), and the second is the so-called semi-gross theory (SGT) in which some parts of the nuclear shell effects are considered. The most recent GT2 and SGT approaches use an updated mass formula, and they better account for the shell and pairing effects [7, 9].

## 3. The gross theory of nuclear neutrino capture (GTNC)

In the most recent versions of $r$-process nucleosynthesis in a supernova, one considers that these processes take place on the surface of a protoneutron star during the supernova collapse. The nuclei are exposed there to a thermal flux $\Phi_\nu(E_\nu)$ of $\nu_\mathrm{e}$ with energy $E_\nu$, which causes the reaction $\nu_\mathrm{e} + (Z, A) \rightarrow (Z+1, A) + \mathrm{e}^-$, with cross-section [10, 12, 19]

$$\langle\sigma_\nu\rangle = \int_{E_{\mathrm{th}}}^{\infty} \Phi_\nu(E_\nu)\sigma_\nu(E_\nu)\,\mathrm{d}E_\nu, \tag{4}$$

where $E_{\mathrm{th}}$ is the reaction energy threshold, which is equal to the $Q_\beta$-value for stable nuclei and zero for unstable cases. For $\Phi_\nu(E_\nu)$ we take a zero-chemical-potential Fermi–Dirac distribution

$$\Phi_\nu(E_\nu) = \frac{\mathcal{N}}{T_\nu^3} \frac{E_\nu^2}{\mathrm{e}^{E_\nu/T_\nu} + 1}, \tag{5}$$

where $T_\nu$ is the neutrino temperature, and $\mathcal{N}$ is the normalization constant of the spectrum [12].

The evaluation of the $\nu_\mathrm{e}$-nucleus cross-section $\sigma_\nu(E_\nu)$, in a neutrino-rich environment, must be consistent with the procedure employed in calculating the $\beta$-decay rates. The allowed transition approximation (see [19], equation (2.19))

$$\sigma_\nu(E_\nu) = \frac{G^2}{\pi} \int_0^{E_\nu - m_\mathrm{e}} p_\mathrm{e} E_\mathrm{e} F(Z+1, E_\mathrm{e}) \left[g_\mathrm{V}^2 |\mathcal{M}_\mathrm{F}(E)|^2 + g_\mathrm{A}^2 |\mathcal{M}_\mathrm{GT}(E)|^2\right] \mathrm{d}E, \tag{6}$$

can be applied for relatively small momentum transfer. The integration covers all possible nuclear states allowed by the selection rules, and the integration limits are determined from

the energy conservation condition. When the energies are measured from the ground state of the parent nucleus $(Z, A)$, this condition reads

$$E_\nu + M(Z, A) = E_e + M(Z+1, A) + Q_{\beta^-} + E, \tag{7}$$

where $E = E_\nu - E_e > 0$ is the excitation energy of the daughter nucleus $(Z+1, A)$, and $F(Z, E)$ is the usual scattering Fermi function which takes into account the Coulomb interaction between the electron and the nucleus.

## 4. Single-particle strength functions

A key element of the gross theory is the single-particle strength probability function $D_X(E)$. The successive improvements of the theory have used Gaussian-, exponential- and Lorentzian-type functions [4, 7]. The sec-hyperbolic functions have been employed in the GT2 [7]. Here, we will mainly adopt the Gaussian-like behavior for the transition strengths. To illustrate that the calculations are rather independent of the functional form adopted for $D_X(E)$, a comparison will be done between the results obtained with the Gaussian-like distribution

$$D_X(E) = \frac{1}{\sqrt{2\pi}\sigma_X} e^{-(E-E_X)^2/(2\sigma_X^2)} \tag{8}$$

and those calculated with the Lorentzian-type strength function

$$D_X(E) = \frac{\Gamma_X}{2\pi} \frac{1}{(E-E_X)^2 + (\Gamma_X/2)^2}. \tag{9}$$

Here $E_X$ is the resonance energy, $\sigma_X$ is the standard deviation, and the other quantities are defined as in [4].

When isospin is a good quantum number, the total Fermi strength $\int |\mathcal{M}_F(E)|\, dE = N - Z$ is carried entirely by the isobaric analog state (IAS) in the daughter nucleus. However, because of the Coulomb force, the isospin is not a good quantum number and this leads to the energy splitting of the Fermi resonance. We will use the estimates introduced by Takahashi and Yamada [4], namely

$$\begin{aligned} E_F &= \pm(1.44 Z A^{-1/3} - 0.7825)\,\text{MeV}, \qquad \text{for } \beta^\pm \text{ decay}, \\ \sigma_F &= 0.157 Z A^{-1/3}\,\text{MeV}. \end{aligned} \tag{10}$$

The total GT strength in the $(\nu_e, e^-)$ channel is given by the Ikeda sum rule $\int |\mathcal{M}_{GT}(E)|\, dE \cong 3(N-Z)$, but its distribution cannot be established by general arguments, and therefore must be either calculated or measured. Charge-exchange reactions (p, n) have demonstrated that most of the strength is accumulated in a broad resonance near the IAS [20]. In fact, even before these measurements were performed, Takahashi and Yamada [4] used the approximation

$$E_{GT} \cong E_F, \tag{11}$$

while $\sigma_{GT}$ is expressed as

$$\sigma_{GT} = \sqrt{\sigma_F^2 + \sigma_N^2}, \tag{12}$$

with $\sigma_N$ being the energy spread caused by the spin-dependent nuclear forces.

For the Fermi transitions, we use the relation (10). Yet, for the GTR, instead of employing the approximation (11), we use the estimate

$$E_{GT} = E_F + \delta,\ \delta = 26 A^{-1/3} - 18.5(N-Z)/A\,\text{MeV}, \tag{13}$$

obtained by Nakayama *et al* [21] from the analytic fit of the (p, n) reaction data of nuclei near the stability line [20], where $\delta$ is positive. For the standard deviation $\sigma_{\rm GT}$ we preserve the expression (12), and $\sigma_{\rm N}$ is treated as an adjustable parameter. Note that the two terms of $\delta$ in (13) have well-defined physical interpretations. The first one is due to the $SU(4)$ symmetry breaking imposed by the spin–orbit coupling, and it is of the same order of magnitude as the Bohr–Mottelson estimate for the spin–orbit splitting ($\Delta_{ls} \cong 20A^{-1/3}$ MeV), obtained from the approximation $l \cong A^{1/3}$ [22]. The second term is responsible for the partial restoration of the $SU(4)$ symmetry, having the same mass and charge dependence as the difference between the energy shifts produced by the GT and Fermi residual interactions. We remark that equation (13) is frequently used in the study of the $r$-process in neutron-rich nuclei [10], [23]–[32]. There $\delta < 0$, and therefore the GTR falls below the IAS, as happens in the shell-model calculation [10].[10]

## 5. Fitting procedure

Another important aspect of the implementation of the GTBD is the choice of the $\chi^2$-minimization method that is used to derive the width parameter $\sigma_N$. In the original work of Takahashi and Yamada [4] the quantity

$$\chi^2_{\rm A} = \sum_{n=1}^{N_0} \left[\log\left(\tau^{\rm cal}_{1/2}(n)/\tau^{\rm exp}_{1/2}(n)\right)\right]^2 \tag{14}$$

is minimized, where $N_0$ is the number of experimental $\beta$-decay half-lives, $\tau^{\rm exp}_{1/2}$, fulfilling the conditions: (i) the branching ratio of the allowed transitions exceeds ~50% of the total $\beta$-decay branching ratio and (ii) the ground-state $Q$-value is $\geqslant 10A^{-1/3}$ MeV.

In the present work, $\sigma_{\rm N}$ is determined through minimization of the function

$$\chi^2_{\rm B} = \sum_{n=1}^{N_0} \left[\frac{\log(\tau^{\rm cal}_{1/2}(n)/\tau^{\rm exp}_{1/2}(n))}{\Delta\log(\tau^{\rm exp}_{1/2}(n))}\right]^2, \tag{15}$$

where

$$\Delta\log(\tau^{\rm exp}_{1/2}(n)) \equiv \left|\log[\tau^{\rm exp}_{1/2}(n) + \delta\tau^{\rm exp}_{1/2}(n)] - \log[\tau^{\rm exp}_{1/2}(n)]\right| \tag{16}$$

and $\delta\tau^{\rm exp}_{1/2}$ is the experimental error. Thus, the $\chi^2_{\rm B}$-function reinforces the contributions of data with small experimental errors. Moreover, we perform different fittings for even–even, odd–odd, odd–even and even–odd nuclei. Needless to say that for $\tau^{\rm exp}_{1/2}$ we use here the most recent data [33], instead of those that were available when the GTBD was formulated [4]. The condition $\log ft \leqslant 6$ is imposed to include only the allowed $\beta$-decays.

[10] Occasionally the fit [7]

$$E_{\rm GT} = E_{\rm F} + \delta', \quad \delta' = 6.7 - 30(N-Z)/A\ \text{MeV}$$

is used, which also reproduces satisfactorily the stable nuclei. The second term of $\delta'$ is interpreted in the same way as that of $\delta$ in (13), but the first term here does not have any direct physical significance.

**Table 1.** Standard deviations $\sigma_N$ (in units of MeV) and mismatch factors $\eta$ for $\beta^-$-decay. Gaussian single-particle strength probability function $D_X(E)$ was adopted. $\sigma_N$ and $\eta$ ($\sigma_N^*$ and $\eta^*$) indicate the results obtained with $E_{GT}$ approximated from equations (13) and (11). The values obtained by Takahashi *et al* [5] for a different data set of nuclei are shown in parentheses. The electronic neutrino cross-section is evaluated with the underlined values of $\sigma_N$.

| $N$–$Z$ (parent) | $N_0$ | $\chi^2_A$ | | | | $\chi^2_B$ | | | |
|---|---|---|---|---|---|---|---|---|---|
| | | $\sigma_N^*$ | $\eta^*$ | $\sigma_N$ | $\eta$ | $\sigma_N^*$ | $\eta^*$ | $\sigma_N$ | $\eta$ |
| Odd–odd | 54 | 13.3 (5.0) | 9.7 (45.5) | 17.6 | 10.7 | 8.6 | 10.6 | <u>15.8</u> | 10.7 |
| Even–even | 43 | 13.5 (4.5) | 9.3 (12.9) | 16.3 | 10.0 | 9.7 | 14.6 | <u>15.8</u> | 10.0 |
| Odd–even | 40 | 13.0 (5.1) | 6.1 (9.4) | 16.8 | 6.4 | 4.1 | 15.6 | <u>7.2</u> | 9.8 |
| Even–odd | 55 | 13.8 (5.1) | 7.3 (6.5) | 17.6 | 7.7 | 10.4 | 7.4 | <u>16.5</u> | 7.7 |

## 6. Numerical results and discussion

### *6.1. $\beta^-$-decay and electron-capture half-lives*

For the single-particle strength probability function, $D_X(E)$, we adopt Gaussian-like behavior (8) in most of the calculations. The corresponding values of the adjustable parameters at the minimal value of the $\chi^2$-function, $\chi^2_{min}$, are listed in table 1 for the four different parity families of nuclei. They are labeled as $\sigma_N^*$ and $\sigma_N$, when equations (11) and (13), respectively, are used for $E_{GT}$. One sees that $\sigma_N$ is always larger than $\sigma_N^*$, which means that the effect of using more realistic energies $E_{GT}$ is reflected in the increase of the standard deviations. The values of $\sigma_N^*$ derived in [4] are exhibited parenthetically in table 1. It is important to point out that the difference between the old and new values for $\sigma_N^*$ does not come from the fitting procedure itself, but from the different samples of nuclei employed here for each parity family.

Figure 1 shows the dependence of $\chi^2/\chi^2_{min}$ on both: (i) the energy of the GTR (left panels for (11) and right panels for (13)) and (ii) the type of minimization function (upper panels for (14) and lower panels for (15)). We note that the $\chi^2_B$-functions present rather pronounced minima when compared with those of the $\chi^2_A$-functions. Moreover, in most cases the $\chi^2_B$ minima are located at smaller values of the standard deviations than the $\chi^2_A$ ones. This is a direct consequence of including the experimental errors in the minimization procedure of the $\chi^2_B$-function.

In order to estimate the average deviation of our results, we have computed the mismatch factor $\eta$ defined as [4]

$$\eta = 10^{\sqrt{\chi^2/N_0}}, \tag{17}$$

showing their values for each $\sigma_N$ in table 1, and similarly the values of $\eta^*$ corresponding to each $\sigma_N^*$. It can be observed that the $\chi^2_B$ minimization procedure considerably reduces the mismatch factor, in particular for the odd–odd family of nuclei. Thus, we can say that the use of the $\chi^2_B$-function modifies $\sigma_N$ and leads to better statistical agreement between the theoretical results and the experimental data.

In figure 2, we compare the experimental $\beta^-$-decay half-lives within the Mn isotopic chain with the results we obtained for the $\sigma_N$ values from table 1. One can see that the GTBD overestimates the data. However, it should be pointed out that this disagreement is not

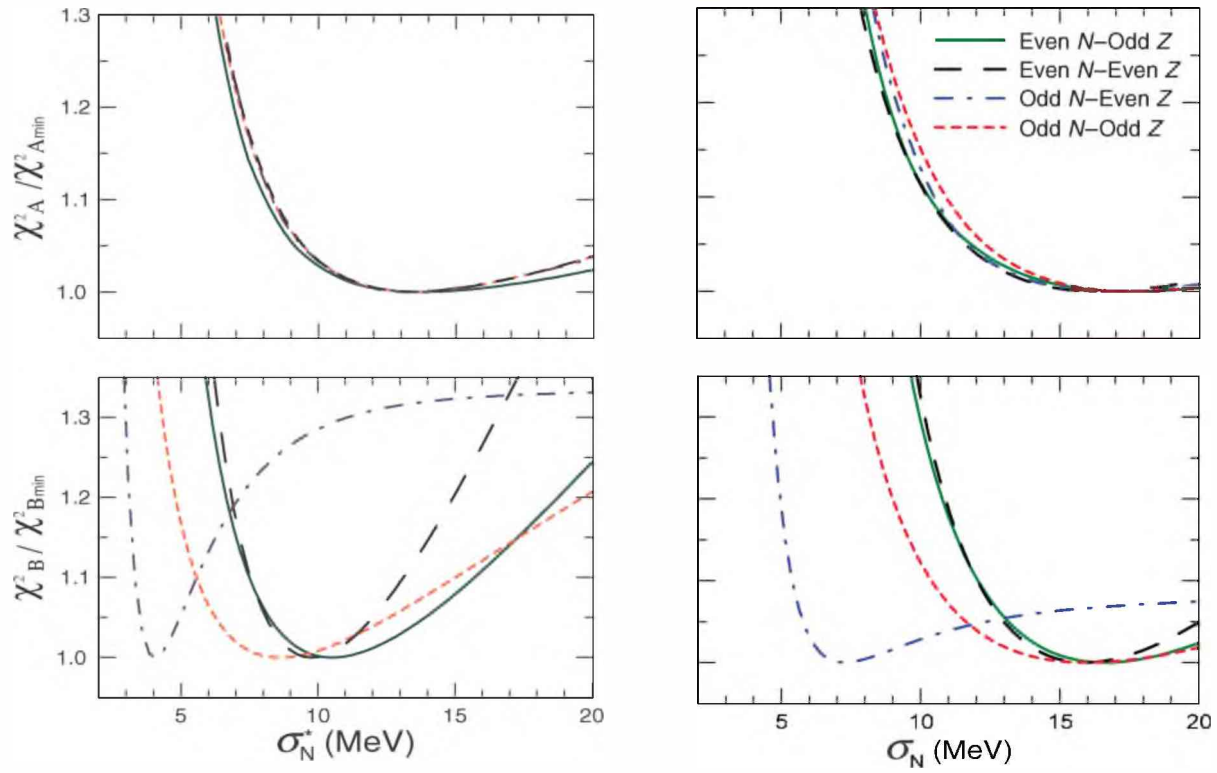


**Figure 1.** Comparison between $\chi^2$ functions (normalized to the minimum) for the $\beta^-$-decay. Two types of approximations were used for the energy of the GTR: the left panel shows the results obtained with the original estimate (11); the right panel includes the energy difference between the GTR and IAS through equation (13).

characteristic of the GTBD, since other microscopic and global models lead to similar results. For instance, this is the case of: (a) the extended Thomas–Fermi plus Strutinsky integral method (ETFSI) combined with the continuum quasiparticle RPA (CQRPA) (ETFSI + CQRPA) [12], and (b) the extended Thomas–Fermi method combined with the semi-gross theory GT2 (ETFSI + GT2) [7].

Figure 3 shows the distribution of $\log(\tau^{\rm cal}_{1/2}/\tau^{\rm exp}_{1/2})$, as a function of $Q_\beta A^{-1/3}$, for $\beta^-$-decay. We observe that the results obtained with equations (11) and (13) are quite similar to each other for the same parity families, the first one being somewhat larger. We can also see that for the odd–odd family very good agreement between theoretical and experimental results is obtained for $Q_\beta A^{1/3} \geqslant 45$ MeV, while for the other three families this happens already for $Q_\beta A^{1/3} \geqslant 40$ MeV. Thus, as frequently mentioned in the literature [4, 7, 9], the best GTBD results are obtained for heavy nuclei.

In the evaluation of the allowed electron-capture and $\beta^+$-decay rates for nuclei of $A < 70$, we have re-adjusted the parameter $\sigma_{\rm N}$, imposing again the constraint $\log ft < 6$. The resulting values of $\sigma_{\rm N}$ and $\eta$ for the two $\chi^2$-functions, with $E_{\rm GT}$ calculated from equation (13), are presented in table 2. Figure 4 shows the values of $\log(\tau^{\rm calc}_{1/2}/\tau^{\rm exp}_{1/2})$ as a function of $Q_\beta A^{1/3}$ for the electron-capture rates calculated with the underlined $\sigma_{\rm N}$ values listed in table 2. Similar general features to those remarked in the $\beta^-$-decay case are obtained.

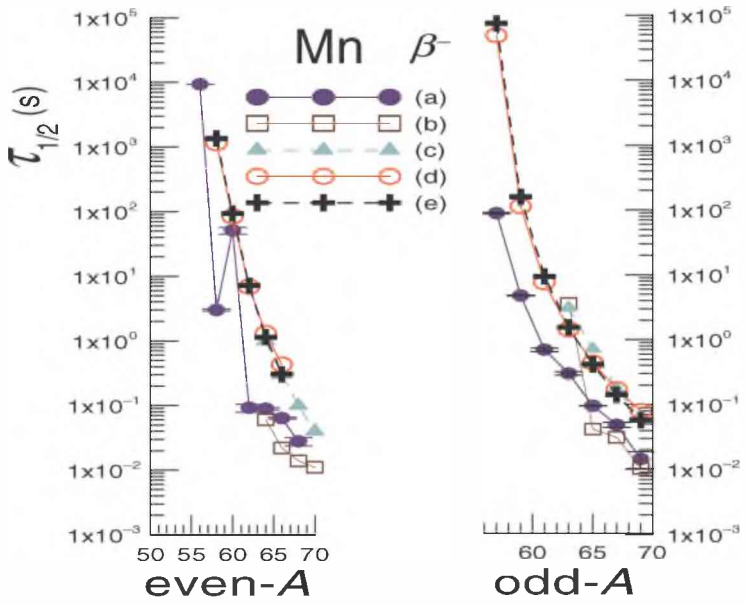


**Figure 2.** Comparison of $\beta^-$-decay half-lives for Mn: (a) experimental; (b) ETFSI + CQRPA [12]; (c) ETFSI + GT2 [7]; (d) GTBD with $E_{\mathrm{GT}}$ from equation (13); and (e) GTBD with $E_{\mathrm{GT}}$ from equation (11). In both GTBD calculations the Gaussian-type functions for $D_{\mathrm{F,GT}}(E)$ were used.

**Table 2.** Standard deviations $\sigma_{\mathrm{N}}$ (in units of MeV) and mismatch factors $\eta$ for $\beta^+$-decay and electron capture. Gaussian single-particle strength function $D_{\mathrm{GT}}$ was used. The energy $E_{\mathrm{GT}}$ has been evaluated from equation (13). The remaining notation is the same as in table 1. No minimum has been found for the $\chi^2_{\mathrm{A}}$-function in the case of even–even parent nuclei.

| $N$–$Z$ (parent) | $N_0$ | $\chi^2_{\mathrm{A}}$ $\sigma_{\mathrm{N}}$ | $\chi^2_{\mathrm{A}}$ $\eta$ | $\chi^2_{\mathrm{B}}$ $\sigma_{\mathrm{N}}$ | $\chi^2_{\mathrm{B}}$ $\eta$ |
|---|---|---|---|---|---|
| Odd–odd | 23 | 9.7 | 10.7 | 10.4 | 10.7 |
| Even–even | 24 | – | – | 9.9 | 5.2 |
| Odd–even | 32 | 12.5 | 6.4 | 11.8 | 9.8 |
| Even–odd | 17 | 12.2 | 7.7 | 12.2 | 7.7 |

Also, we briefly discuss the dependence of the $\chi^2$ procedure on the functional form of the employed strength distribution. Thus, we repeat the calculations for $\beta^-$-decay and electron-capture rates using now the Lorentzian distribution $D_\chi$, given by equation (9), together with equation (13) for the GT energy. The resulting $\Gamma_{\mathrm{N}}$ energies are shown in table 3, and the corresponding $\log(\tau^{\mathrm{calc}}_{1/2}/\tau^{\mathrm{exp}}_{1/2})$ values for the $\beta^-$ emitter nuclei with $A < 70$ exhibit similar $Q_\beta A^{1/3}$ dependence to that shown in figure 3.

Figure 5 shows the results for the electron-capture rates along the Ni isotopic chain. The calculations with the Gaussian and Lorentzian strength functions turn out to be quite similar to each other and both show reasonable agreement with the data.

**Table 3.** Standard deviations $\sigma_N$ (in units of MeV) and mismatch factors $\eta$ for $\beta^-$-decay and electron capture, obtained from the minimization of the $\chi^2_B$-function. A Lorentzian single-particle strength probability function was used. The energy $E_{GT}$ has been evaluated from equation (13).

| $N$–$Z$ (parent) | $\beta^-$-decay | | | e$^-$-capture | | |
|---|---|---|---|---|---|---|
| | $N_0$ | $\Gamma_N/2$ | $\eta$ | $N_0$ | $\Gamma_N/2$ | $\eta$ |
| Odd–odd | 54 | 15.2 | 12.7 | 23 | 9.8 | 11.3 |
| Even–even | 43 | 15.4 | 11.6 | 24 | 9.4 | 6.5 |
| Odd–even | 40 | 8.5 | 8.0 | 32 | 11.3 | 6.4 |
| Even–odd | 55 | 15.7 | 8.6 | 17 | 11.5 | 8.0 |

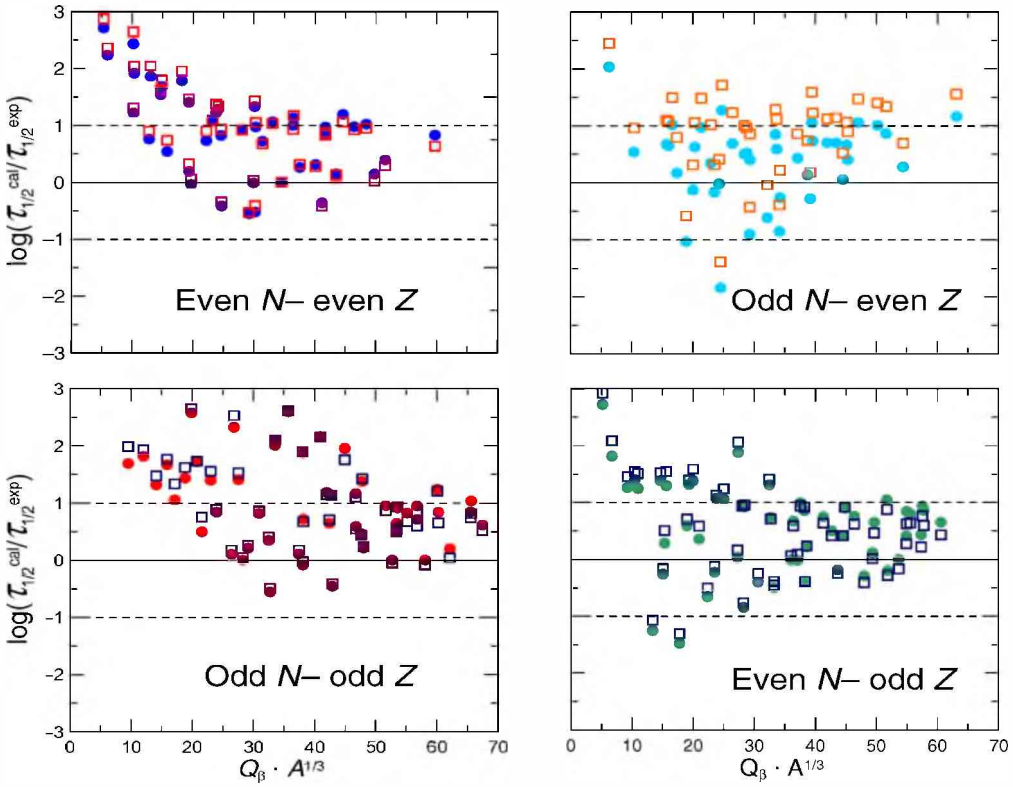


**Figure 3.** $\log(\tau^{calc}_{1/2}/\tau^{exp}_{1/2})$ as a function of $Q_\beta A^{1/3}$ for $\beta^-$-decay of nuclei with $A < 70$. Gaussian functions were used for $D_X(E)$. We present the values obtained with the approximations (13) (filled circles) and (11) (open squares) for $E_{GT}$.

### 6.2. *Neutrino-nucleus cross-section*

The reduced thermal cross-section $\langle\sigma_\nu\rangle/A$ of the four $\beta^-$ emitter families was evaluated for the $A < 70$ nuclei with two sets of parameters, $\sigma^*_N$ and $\sigma_N$. The results, shown in figure 6, indicate that equation (13) always yields smaller values for this quantity to those obtained with equation (11), the difference being more pronounced for $A > 30$. However, for some isolated

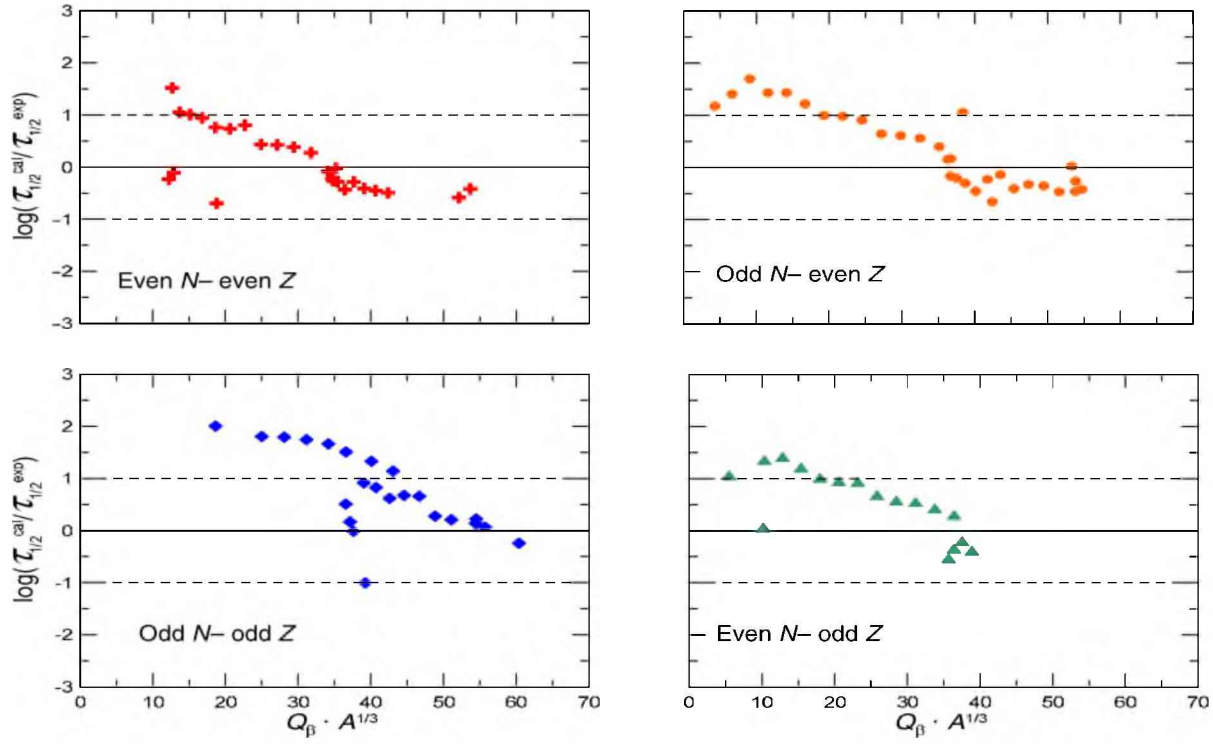


**Figure 4.** $\log(\tau_{1/2}^{\mathrm{calc}}/\tau_{1/2}^{\mathrm{exp}})$ as a function of $QA^{1/3}$ for electron capture of nuclei with $A < 70$. Gaussian functions were used for $D_X(E)$ and $E_{\mathrm{GT}}$ was calculated from equation (13).

light nuclei, the use of a more realistic GTR energy increases the cross-section. This is the case of $^{12}$B, for which the product $\sigma(E_\nu)\Phi(E_\nu)$ is shown in the left panel of figure 7. The increase of $\sigma(E_\nu)$ arises from the contribution of the $1^+$ states with energies below the GTR (see [19, 34]). As another example, the results for the Ni isotopes ($^{67}$Ni, $^{68}$Ni and $^{69}$Ni) are shown in the right panel of figure 7. Note that for the three nuclei, the product $\sigma(E_\nu)\Phi(E_\nu)$ will decrease if the energy of the GTR is raised. Also, because of the pairing effect, the cross-section in $^{68}$Ni presents the lowest value for both the GT energies.

On the other hand, from figure 8 it can be seen that our results for the reduced thermal cross-section in Ni nuclei emphasize the odd–even effect when compared with the microscopic ETFSI + CQRPA calculations [12], where this effect seems to have been removed. This leads to a different trend of the $\nu_e$-nucleus cross-section with respect to $A$.

For completeness, in figure 9 we present the results for $\langle\sigma_\nu\rangle/A$ obtained with the GTNC, both for the $\beta^-$-decaying nuclei (with $\sigma_{\mathrm{N}}$ from table 1) and for the nuclei where electron capture takes place (with $\sigma_{\mathrm{N}}$ from table 2).

It is worth noticing that the Gaussian and Lorentzian strength functions given, respectively, by equations (8) and (9) yield almost the same results for the reduced thermal cross-sections.

At this point, it is important to clarify the meaning of the thermal neutrino flux presented in equation (5), which we have used for the calculation of the thermal neutrino-nucleus cross-section $\langle\sigma_\nu\rangle$. This neutrino energy flux is given by a Fermi distribution, i.e. equation (5), depending explicitly on the temperature parameter $T_\nu$. In order to compare our results with

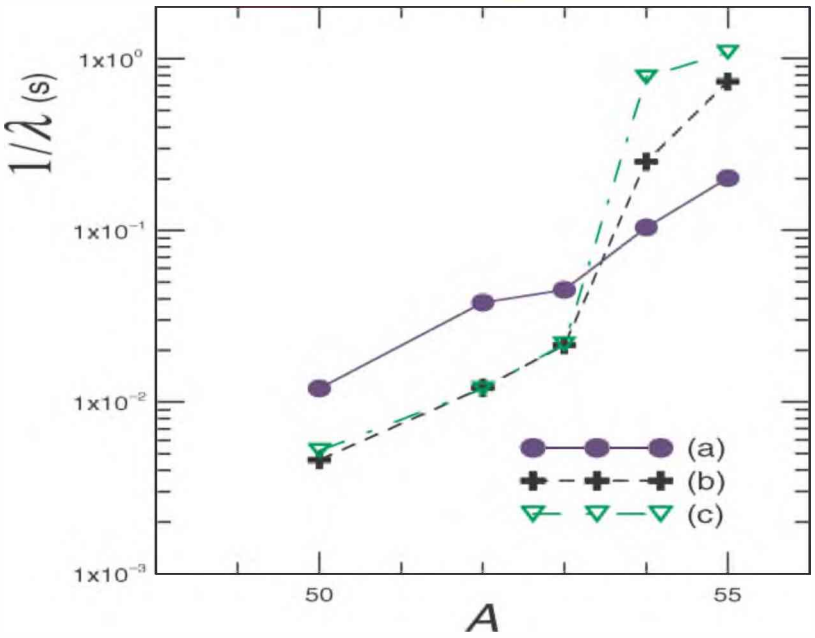


**Figure 5.** Electron-capture rates for Ni isotopic chain: (a) experimental; (b) GTBD with Gaussian-type function; and (c) GTBD with Lorentzian-type function. The energy of the GTR was approximated by equation (13).

those of Borzov and Goriely [12], we have used here a constant temperature $T_\nu = 4\,\mathrm{MeV}$. However, this situation could not be a realistic one for the supernova neutrino wind. Neutrinos (and antineutrinos) with different energies and flavors decouple at different points of the supernova core and the neutrino spectrum, in fact, could be non-thermal. This is due to the non-thermalization of neutrinos through their transport along hydrodynamics medium evolution [35, 36]. Thus, it could be interesting to determine the consequences of employing a different neutrino flux such as a power law flux of the form

$$\Phi_\nu(E_\nu) = \mathcal{N}_{\mathrm{PL}} \left( \frac{\epsilon_\nu}{\langle \epsilon_\nu \rangle} \right)^{\alpha} \mathrm{e}^{-[(\alpha+1)\epsilon_\nu/\langle \epsilon_\nu \rangle]}. \tag{18}$$

The parameters $\langle \epsilon_\nu \rangle$ and $\alpha$ are not fully determined and here we take $\langle \epsilon_\nu \rangle \approx 3.1514 T_\nu = 12.6056\,\mathrm{MeV}$, and $\alpha \approx 2.3014$, which reproduces better the Fermi–Dirac neutrino distribution function in equation (5) using $T_\nu = 4\,\mathrm{MeV}$. These parameter values were obtained in [35]. The normalization constant $\mathcal{N}_{\mathrm{PL}}$ ensures unitary flux between 0 and 102 MeV. We have found that, for all practical purposes, the flux (18) yields the same results as the thermal flux (5). This is an expected result, since these two fluxes tend to behave differently only in the tail zone, far away from the integration interval used to obtain the $\sigma_\nu(E)$ for astrophysical applications. Some possible deviations in the tail of these fluxes are important for the rate of nuclear reactions in studies of astrophysics plasmas [37].

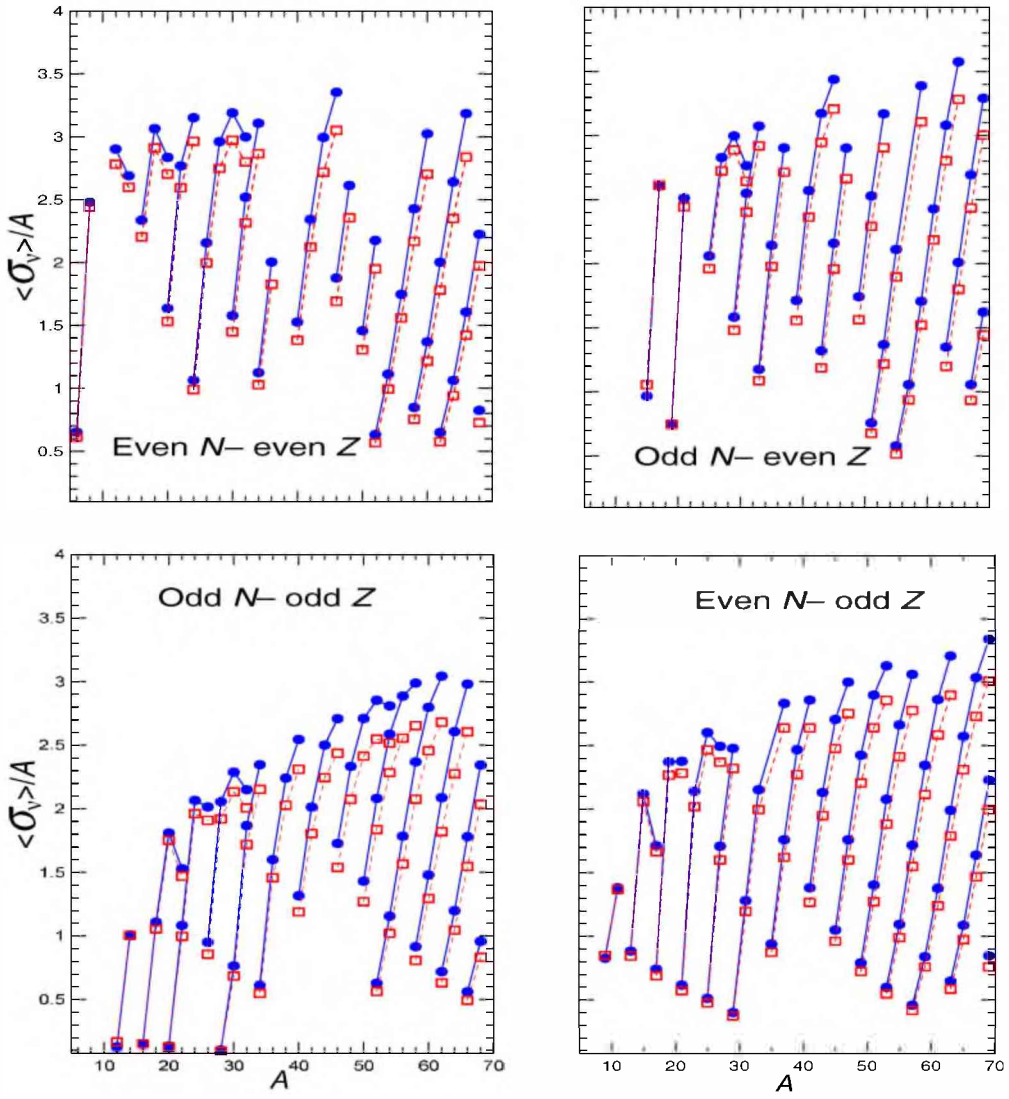


**Figure 6.** Thermal reduced $\nu_e$-nucleus cross-section $\langle\sigma_\nu\rangle/A$ (in units of $10^{-40}\,\mathrm{cm}^2$) for $\beta^-$ emitters with $A < 70$. Gaussian functions were used for $D_X(E)$. Results obtained with both approximations for the GTR are presented, with parameter values given by equation (11) (filled circles) and by equation (13) (open squares).

## 7. Conclusions

We have briefly reviewed the original version of the gross theory for $\beta$-decay. The main improvement introduced is a more realistic estimate of the location of the GTR energy peak, $E_{\mathrm{GT}}$. After fixing the free parameter of our model ($\sigma_{\mathrm{N}}$ or $\Gamma_{\mathrm{N}}$, depending on the parameterization adopted for the strength function), we have calculated the $\beta^-$-decay and electron-capture rates. A careful selection of input data for $A < 70$ nuclei, with small error bars in the measured half-lives, has been done in order to fix the model parameters in the fitting procedure. The model can be extended to the $A > 70$ nuclei, as well as to the transuranic nuclei, which are of interest for the study of the $r$-process

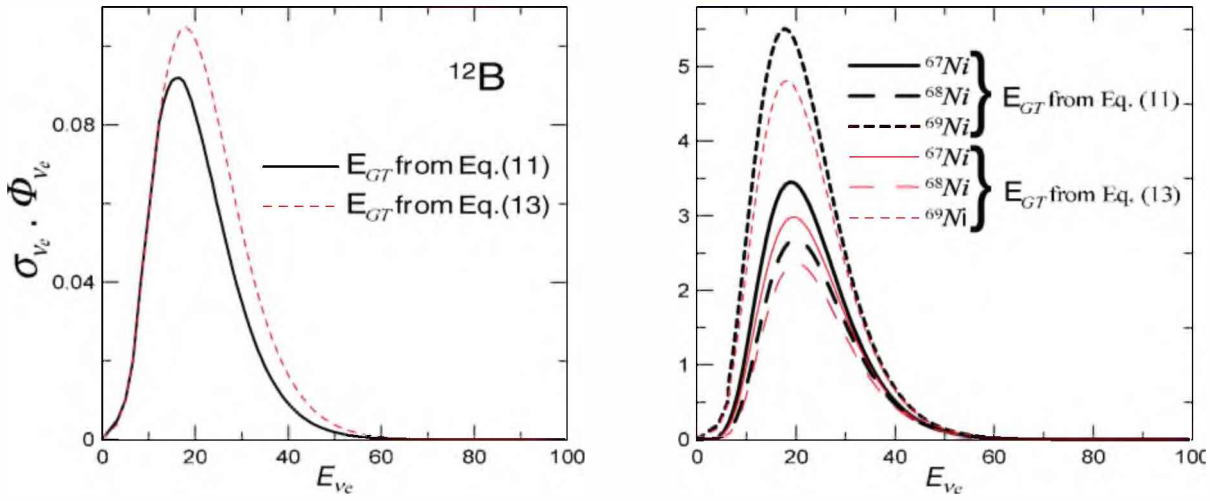


**Figure 7.** Results for $\sigma(E_\nu)\Phi(E_\nu)$ (in units of $10^{-42}$ cm$^2$ MeV$^{-1}$). Gaussian functions were used for $D_X(E)$, and the results with both (11) and (13) approximations for $E_{\rm GT}$ are shown, for $^{12}$B (left panel) and for $^{67,68,69}$Ni isotopes (right panel).

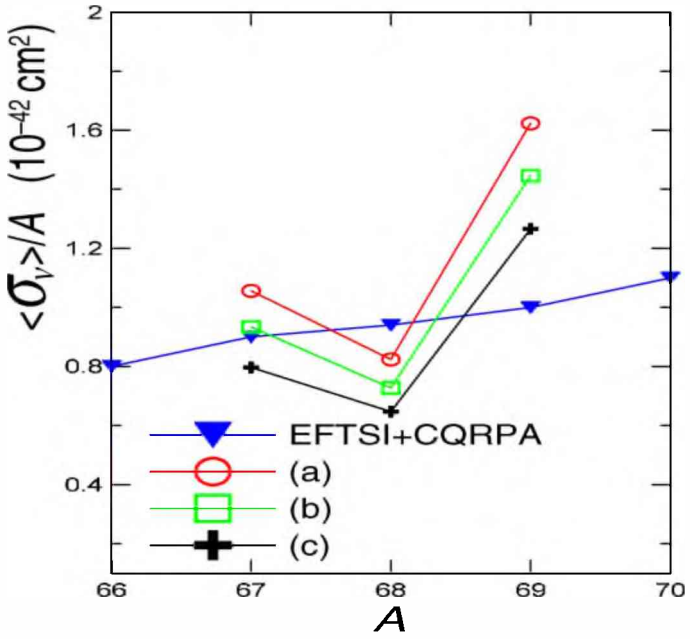


**Figure 8.** Comparison between microscopic ETFSI + CQRPA calculation from [12] and our GTNC results for the electronic thermal reduced neutrino cross-section (in units of $10^{-42}$ cm$^2$) for some Ni isotopes. The results obtained with Gaussian strength functions are shown in (a) with $E_{\rm GT}$ from (11) and in (b) with $E_{\rm GT}$ from (13). The calculations with Lorentzian distribution and $E_{\rm GT}$ from (13) are shown in (c).

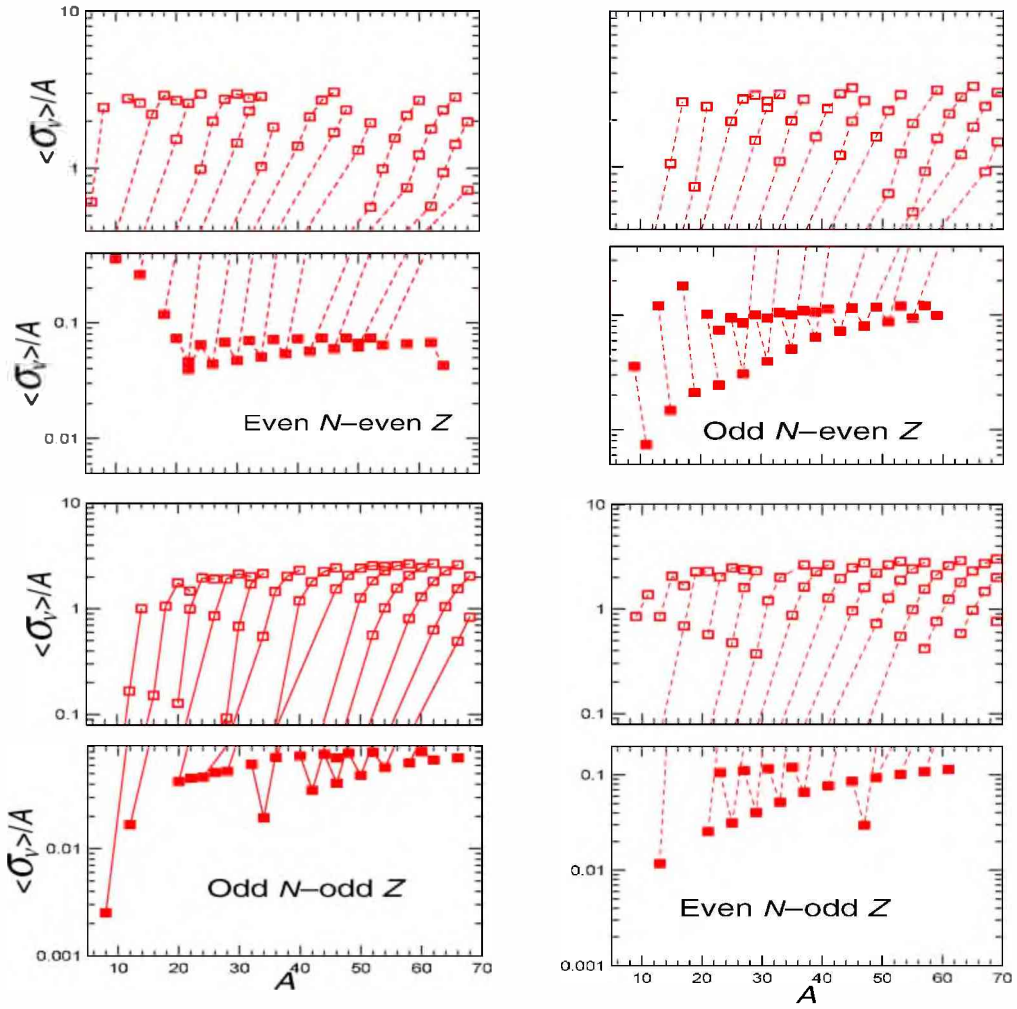


**Figure 9.** Thermal reduced $\nu_e$-nucleus cross-section (in units of $10^{-40}$ cm$^2$) for the $A < 70$ region with the neutrino flux at $T_\nu = 4$ MeV. Equation (13) for $E_{GT}$ was used together with the Gaussian strength function. We present the results for electron capture (filled squares) and $\beta^-$ emitters (open squares).

in a supernova. The first- and second-forbidden weak processes could play an important role in the exotic nuclei within this nuclear mass region. But these transitions can be easily included in the gross theory framework, as has already been done by Nakata *et al* [10] within the SGT[11].

The present results are encouraging, in the sense that the gross theory is able to describe in a systematic way not only the nuclear properties along the $\beta$-stability line but also exotic nuclei involved in presupernova composition. In particular, the results for the reduced thermal cross-section $\langle\sigma_\nu\rangle/A$ in the region $A < 70$ are in fair agreement with previous calculations performed within more refined microscopic models, i.e. the ETFSI + CQRPA model [12]. The difference

[11] A relation analogous to (13) was also derived for the first forbidden charge-exchange resonances [38], which is quite different from the one used in [9]. Thus, it might be more appropriate to employ [38, equations (3.11) and (3.12)] than [9, equation (48)].

between the two descriptions could be attributed to the use of the Fermi gas model, which contains more degrees of freedom than the EFTSI + CQRPA model. Consequently, in general, $\sigma_\nu(E_\nu)$ calculated with the Fermi gas model leads to values higher than those obtained with microscopical nuclear models [39]–[41], particularly for light or intermediate nuclei (see, for instance, the results for the $\nu-^{12}$C reaction shown in [9, figure 2] and [41, figure 32]).

An important aspect of the recent $r$-process calculations is that they take into account the neutrino-rich environment in supernova explosions, where the $\nu_e$-nucleus reaction is in competition with $\beta$-decay processes [42]. To address this type of calculation we have evaluated the cross-section $\sigma_{\nu_e}(E_\nu)$ within the GTNC model, folded with a temperature-dependent neutrino flux.

Finally, we want to note once more the simplicity of the present model, which we are planning to extend in the near future to the $r$-process nuclei region, as well as to evaluate the isotopic abundance in the presupernova scenario.

## Acknowledgments

ARS acknowledges financial support from FAPERJ (Rio de Janeiro, Brasil) and Texas A&M University—Commerce. Two of us (CAB and FK) are members of CONICET (Argentina). SBD acknowledges partial support from CNQq, Brazil. FK acknowledges support from FAPESP (São Paulo, Brazil). We thank C Bertulani for a careful reading and revision of the manuscript.

## References

[1] Goriely S, Demetriou P, Janka H-Th, Pearson J M and Samyn M 2005 *Nucl. Phys.* A **758** 587
Arnould M, Goriely S and Takahashi K 2007 *Phys. Rep.* **450** 97
[2] Hillebrandt W 2002 *Eur. Phys. J.* A **15** 53
[3] Borzov I N and Goriely S 2003 *Preprint* http://www1.jinr.ru/Archive/Pepan/2003-v34/v-34-6/pdf_obzory/v34p6_01.pdf
[4] Takahashi K and Yamada M 1969 *Prog. Theor. Phys.* **41** 1470
[5] Koyama S, Takahashi K and Yamada M 1970 *Prog. Theor. Phys.* **44** 663
[6] Kondoh T, Tachibana T and Yamada M 1985 *Prog. Theor. Phys.* **74** 708
[7] Tachibana T, Yamada M and Yoshida Y 1990 *Prog. Theor. Phys.* **84** 641
[8] Tachibana T, Yamada M and Yoshida N 1992 *Prog. Theor. Phys.* **84** 641
[9] Nakata H, Tachibana T and Yamada M 1997 *Nucl. Phys.* A **625** 521
[10] Qian Y Z, Haxton W C, Langanke K and Vogel P 1997 *Phys. Rev.* C **55** 1532
[11] Langanke K 1999 *Phys. Rev. Lett.* **83** 4502
Martinez-Pinedo G 2000 *Nucl. Phys.* A **668** 357
Langanke K 2006 *Phys. Scr.* T **125** 26
[12] Borzov I N and Goriely S 2000 *Phys. Rev.* C **62** 035501
[13] Goriely S and Khan E 2002 *Nucl. Phys.* A **706** 217
[14] Itoh N, Kohyama Y and Fujii A 1997 *Nucl. Phys.* A **287** 501
Itoh N and Kohyama Y 1997 *Nucl. Phys.* A **306** 527
[15] Feenberg E and Trigg G 1950 *Rev. Mod. Phys.* **22** 399
[16] Rose M E (ed) 1960 Relativistic Electron Theory (New York: Wiley) chapter V
Brysk H and Rose M E 1958 *Rev. Mod. Phys.* **30** 1169
[17] Wapstra A H, Audi G and Hoekstra R 1988 *At. Data Nucl. Data Tables* **39** 281
[18] Tachibana T, Uno M, Yamada M and Yamada S 1988 *At. Data Nucl. Data Tables* **39** 251

[19] Krmpotić F, Samana A and Mariano A 2005 *Phys. Rev.* C **71** 044319
[20] Horen D J *et al* 1980 *Phys. Lett.* B **95** 27
Horen D J *et al* 1981 *Phys. Lett.* B **99** 383
Gaarde C *et al* 1981 *Nucl. Phys.* A **369** 258
[21] Nakayama K, Galeão A P and Krmpotić F 1982 *Phys. Lett.* B **114** 217
Nakayama K, Galeão A P and Krmpotić F 1983 *Nucl. Phys.* A **399** 478
[22] Bohr A and Mottelson B R 1975 *Nuclear Structure* vol 2 (New York: Benjamin)
[23] Bender M *et al* 2002 *Phys. Rev.* C **65** 054322
[24] Langanke K and Martinez-Pinedo G 2000 *Nucl. Phys.* A **673** 481
[25] Surman R and Engel J 1998 *Phys. Rev.* C **58** 2526
[26] Kar K *et al* 1998 *J. Phys. G: Nucl. Part. Phys.* **24** 1641
[27] Sutaria F K and Ray A 1995 *Phys. Rev.* C **52** 3460
[28] Kar K and Sarkar S 1994 *Astrophys. J.* **434** 662
[29] Dean D J *et al* 1994 *Phys. Rev. Lett.* **72** 4066
[30] Kar K, Sarkar S and Ray A 1991 *Phys. Lett.* B **261** 217
[31] Cooperstein J and Wambach J 1984 *Nucl. Phys.* A **420** 591
[32] Hektor A *et al* 2000 *Phys. Rev.* C **61** 055803
[33] Pritychenko B 2006 *Nuclear Wallet Cards* online at http://www.nndc.bnl.gov/wallet
[34] Samana A and Krmpotić F 2006 *Ann. XXVIII Workshops in Nuclear Physics in Brazil* (São Paulo: Livraria da Física)
[35] Keil M, Raffel G G and Hanka H-T 2003 *Astrophys. J.* **590** 971
[36] Jachowicz N and McLaughlin G C 2006 *Phys. Rev. Lett.* **96** 172301
[37] Lissia M and Quarati P 2005 *Europhys. News* **36** 211
[38] Krmpotić F, Nakayama K and Galeão A P 1983 *Nucl. Phys.* A **339** 475
[39] Moniz E J 1969 *Phys. Rev.* **184** 1154
Smith R A and Moniz E J 1972 *Nucl. Phys.* B **43** 605
[40] Kolbe E, Langanke K and Krewald S 1994 *Phys. Rev.* C **49** 1122
[41] Athanassopulus C *et al* 1998 *Phys. Rev.* C **58** 2489
Athanassopulus C *et al* 1998 *Phys. Rev. Lett.* **81** 1774
[42] Terasawa M, Langanke K, Kajino T and Mathews G J 2004 *Astrophys. J.* **608** 470